



# Modeling slug tests in unconfined aquifers taking into account water table kinematics, wellbore skin and inertial effects

Bwalya Malama<sup>a,\*</sup>, Kristopher L. Kuhlman<sup>a</sup>, Warren Barrash<sup>b</sup>, Michael Cardiff<sup>b</sup>, Michael Thoma<sup>b</sup>

<sup>a</sup> Sandia National Laboratories, 4100 National Parks Hwy, Carlsbad, NM 88220, USA

<sup>b</sup> CGISS & Department of Geosciences, Boise State University, Boise, ID, USA

## ARTICLE INFO

### Article history:

Received 11 January 2011

Received in revised form 27 May 2011

Accepted 19 July 2011

Available online 27 July 2011

This manuscript was handled by Philippe Baveye, Editor-in-Chief, with the assistance of Thomas J. Burbey, Associate Editor

### Keywords:

Slug tests

Unconfined aquifer

Skin

Hydraulic conductivity

Specific storage

Specific yield

## ABSTRACT

Two models for slug tests conducted in unconfined aquifers are developed by (a) extending the unconfined KGS solution to oscillatory responses, yielding a model referred to herein as the unified model, and (b) replacing the constant head condition with the linearized kinematic condition at the water table. The models can be used to analyze the full range of responses from highly oscillatory to overdamped. The second model, referred to as the moving water table (MWT) model, is only applicable when effects of well bore skin are negligible. The models are validated by comparison with published solutions, and by application to a published case study of field tests conducted in wells without skin in an unconfined aquifer at the MSEA site in Nebraska. In this regard (a) the MWT model essentially yields the same results as the confined KGS model, except very close to the water table, and (b) the unified model yields slightly smaller aquifer  $K$ -values relative to the MWT model at all positions in the well. All model solutions yield comparable results when fitted to published field data obtained in an unconfined fluvial aquifer at the MSEA site in Nebraska. The unified model is fitted to field data collected in wells known to exhibit positive skin effects at the Boise Hydrogeophysical Research Site (BHRS) in Boise, Idaho. It is shown to yield hydraulic conductivity estimates of comparable magnitude to those obtained with the KGS model for overdamped responses, and the Springer–Gelhar model for oscillatory responses. Sensitivity of the MWT model to specific yield,  $S_y$ , and hydraulic anisotropy,  $\kappa$  is evaluated and the results, when plotted in log–log space and with consideration of log-scale time derivatives of the response, indicate that these two parameters should be estimable from slug test data, though challenges still remain.

© 2011 Elsevier B.V. All rights reserved.

## 1. Introduction

Slug tests are widely used in aquifer characterization since they can be performed quickly, and require less equipment and labor than other methods such as pumping and injection tests. Additionally, they do not produce water, which may be contaminated and require costly disposal. They can be conducted by immersing or removing a slug mass into or from a well (Cooper et al., 1967), by instantaneous injection of water using a high-pressure pump (Bredehoeft and Papadopoulos, 1980), or by instantaneous application or removal of pressurized gas to the water column in a well (Butler, 1998). All three approaches involve the near-instantaneous raising or lowering of hydraulic head in a source well and observing its recovery, for single well tests, or observing the response in another well, for multi-well tests.

Mathematical solutions to the slug test flow problem for both confined and unconfined aquifers are available in the hydrogeology

literature (e.g., Butler, 1998). The solution of Hyder et al. (1994), referred to hereafter as the KGS solution, was developed to analyze slug tests in confined and unconfined aquifers, incorporating wellbore skin and storage effects. However, it does not account for wellbore inertial effects that are manifested by oscillatory head responses in the source well. Other models for unconfined aquifers, such as those of Springer and Gelhar (1991) (referred to as SG) and Zlotnik and McGuire (1998) (referred to as ZM), account for inertial effects but not for the presence of a filter pack around the source wellbore or for formation storage. Hence, there is a need for a unified solution that accounts for inertial, skin (or filter-pack) and storage effects for analyzing slug tests performed in unconfined aquifers. For confined aquifers, the solution of Butler and Zhan (2004), referred to herein as the BZ model, serves this purpose.

In modeling flow to a pumping well in unconfined aquifers, it is common to model the water table as a moving boundary and use a linearized form of the kinematic condition as the boundary condition at the water table (Neuman, 1972; Moench, 1997). However, when modeling slug tests in such aquifers, owing to the rapidity of the dissipation and relatively small magnitude of the initial slug, it is common to impose a Dirichlet-type (constant head) boundary

\* Corresponding author. Tel.: +1 575 234 0107; fax: +1 575 234 0061.

E-mail address: [bnmalam@sandia.gov](mailto:bnmalam@sandia.gov) (B. Malama).

<sup>1</sup> Formerly at Montana Tech of the University of Montana, Butte, MT, USA

## Nomenclature

|                |   |        |  |
|----------------|---|--------|--|
| $K_{r,i}$      | radial hydraulic conductivity of $i$ th zone ( $L T^{-1}$ )   | $b$    | length of test interval (L)  |
| $K_{z,i}$      | vertical hydraulic conductivity of $i$ th zone ( $L T^{-1}$ ) | $d$    | depth to top of test interval (L)  |
| $S_{s,i}$      | specific storage of $i$ th zone ( $L^{-1}$ )                  | $l$    | depth to bottom of test interval (L)   |
| $S_y$          | specific yield (–)  | $s_i$  | head change in $i$ th zone (L)   |
| $\alpha_{r,i}$ | hydraulic diffusivity of $i$ th zone ( $L^2 T^{-1}$ )         | $H$    | displacement from equilibrium position in source well (L)                        |
| $B$            | aquifer thickness (L)   | $H_0$  | initial slug input (L)   |
| $z$            | vertical distance, measured down from water table (L)         | $H'_0$ | initial velocity of slug input ( $L T^{-1}$ )                                    |
| $r$            | radial distance from center of source well (L)                | $T_c$  | characteristic time ( $T_c = B^2/\alpha_{r,1}$ ) (T)                             |
| $t$            | time since slug initiation (T)                                | $\nu$  | kinematic viscosity of water ( $L^2 T^{-1}$ )                                    |
| $r_w$          | radius of source well at test interval (L)                    | $g$    | acceleration due to gravity ( $L T^{-2}$ )                                       |
| $r_c$          | radius of slug test tubing (L)                                | $p$    | Laplace transform parameter, $\bar{f}(p) = \int_0^\infty f(t_D) e^{-p t_D} dt_D$ |
| $r_s$          | radial extent of filter pack (L)                              | $a$    | Hankel transform parameter, $f(a) = \int_0^\infty a f(r_D) J_0(ar_D) dr_D$       |
| $C_w$          | coefficient of wellbore storage ( $L^2$ )                     |        |  |

condition at the water table (Bouwer and Rice, 1976; Hyder et al., 1994). The effect of a moving water table condition on slug test response has never been investigated, nor has the potential for using slug tests to estimate specific yield.

This work addresses the deficiencies of available unconfined aquifer slug test models by (a) extending the KGS model to slug test problems where inertial effects are significant, and (b) developing a solution that incorporates water table kinematics into the model. The latter is based on the use of the linearized kinematic condition of Neuman (1972) as the water-table boundary condition. Inertial effects are treated using the simplified momentum balance equation of Butler and Zhan (2004); that is, nonlinear dissipative processes associated with fittings and flow path constrictions inside the well, as discussed in McElwee and Zenner (1998), and Zenner (2009), are neglected. The unified solution presented herein is applicable to both monotonic and oscillatory responses, but, like the KGS model, it cannot be used close to the water table, due to the constant head assumption at the water table. The use of the linearized kinematic condition obviates this limitation for wells with negligible skin effects, and leads to a solution that can be used to analyze data collected anywhere along a well emplaced in a water table aquifer.

The unified and MWT solutions are validated through comparison against published solutions, and by application to a published case study of field tests conducted in wells without skin in an unconfined aquifer at the MSEA site in Nebraska (Zlotnik and McGuire, 1998). The unified model is used to estimate formation hydraulic parameters from slug test data collected in wells with positive skin at the Boise Hydrogeophysical Research Site (BHRS) in Boise, Idaho. Additionally, an empirical analysis of the sensitivity of hydraulic conductivity estimates to skin radial extent and hydraulic conductivity is presented. Sensitivity of the MWT model to specific yield,  $S_y$ , and hydraulic anisotropy,  $\kappa$  is also evaluated and the results, when plotted in log–log space, indicate that these two parameters should be estimable from slug test data. Data are presented from a site near Butte, Montana, that show possible evidence of water table movement. The use of derivatives is also suggested as a possible approach to enhancing identifiability of  $S_y$  and  $\kappa$ .

## 2. Mathematical formulation

The mathematical formulation of the slug test problem considered here is based on the following (nonexhaustive) list of assumptions:

1. Aquifer (and skin or filter pack) is homogeneous but anisotropic;

2. Aquifer is of infinite radial extent;
3. Wellbore has storage and finite skin (filter pack);
4. Nonlinear effects in the wellbore are negligible;
5. Water table boundary condition is constant head of Hyder et al. (1994) or the linearized kinematic condition of Neuman (1972); and
6. Aquifer is bounded from below by an impermeable layer.

The governing equation for flow in the aquifer formation and wellbore skin (filter pack or disturbed zone around wellbore) is given by

$$S_{s,i} \frac{\partial s_i}{\partial t} = \frac{K_{r,i}}{r} \frac{\partial}{\partial r} \left( r \frac{\partial s_i}{\partial r} \right) + K_{z,i} \frac{\partial^2 s_i}{\partial z^2} \quad (1)$$

where  $i = 1$  for skin and  $i = 2$  for the formation,  $s_i$  is change in head from the initial static level in the  $i$ th flow zone,  $K_{r,i}$  and  $K_{z,i}$  are the radial and vertical hydraulic conductivities in the  $i$ th flow zone,  $S_{s,i}$  is the specific storage of the  $i$ th flow zone, and  $(r, z, t)$  are the space–time coordinates. The  $z$ -coordinate is positive downward from the water table ( $z = 0$ ) into the formation. A schematic of the flow domain is shown in Fig. 1. Eq. (1) is solved subject to the zero initial condition

$$s_i(r, z, 0) = 0, \quad (2)$$

and the no-flow boundary condition at the base of the aquifer, namely,

$$\left. \frac{\partial s_i}{\partial z} \right|_{z=B} = 0, \quad (3)$$

where  $B$  is the initial saturated thickness of the aquifer. The boundary condition at  $z = 0$  (the water table) will be specified in

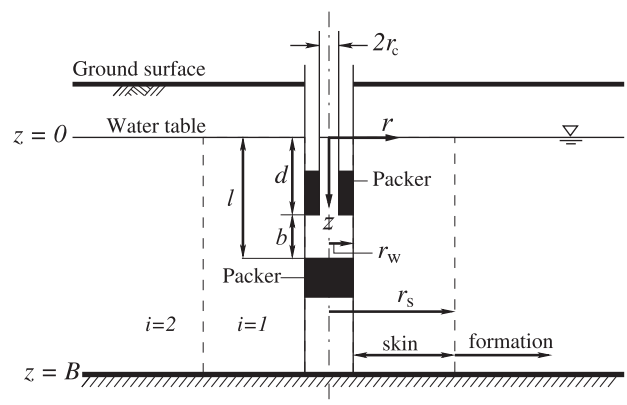


Fig. 1. Schematic of the slug-test problem flow domain.

subsequent sections where the distinction between the moving water table and the constant head conditions is made.

For the formation, the Dirichlet boundary condition given by

$$\lim_{r \rightarrow \infty} s_2(r, z, t) = 0, \quad (4)$$

is imposed at an infinitely far radial distance from the wellbore. The continuity head and flux conditions given by

$$s_1(r_s, z, t) = s_2(r_s, z, t), \quad (5)$$

and

$$K_{r,1} \frac{\partial s_1}{\partial r} \bigg|_{r=r_s} = K_{r,2} \frac{\partial s_2}{\partial r} \bigg|_{r=r_s}, \quad (6)$$

are imposed at  $r_s$ , the radial distance to the outer limit of the filter pack.

A mass balance condition is imposed across the test interval at the source well

$$2\pi b K_{r,1} \left( r \frac{\partial s_1}{\partial r} \right) \bigg|_{r=r_w} = \begin{cases} C_w \frac{dH}{dt} & \forall z \in [d, l] \\ 0 & \text{elsewhere,} \end{cases} \quad (7)$$

where  $H(t)$  is head in the wellbore, subject to the initial condition

$$H(t=0) = H_0. \quad (8)$$

$r_w$  is well screen radius,  $d$  and  $l$  are the depths from the water table to the top and bottom of the test interval, respectively,  $b$  is the length of the test interval,  $C_w = \pi r_c^2$  is the coefficient of wellbore storage,  $r_c$  is the tubing radius in the part of the tubing where the water column is pressurized, and  $H_0$  is the initial slug input that drives the system response.

To model oscillatory responses, inertial effects are accounted for by applying the principle of momentum conservation in the source well, leading to (Butler and Zhan, 2004)

$$\frac{d^2 H(t)}{dt^2} + \frac{8\nu L}{r_c^2 L_e} \frac{dH(t)}{dt} + \frac{g}{L_e} H(t) = \frac{g}{b L_e} \int_d^l s_1(r_w, z, t) dz, \quad (9)$$

where  $\nu$  is the kinematic viscosity of water,  $g$  is the acceleration due to gravity,  $L$  is a length parameter defined in Butler (2002) as

$$L = d + \frac{b}{2} \left( \frac{r_c}{r_w} \right)^4,$$

and  $L_e$  is the effective length of the water column in the well, defined in Kipp (1985) and Zurbuchen et al. (2002) as

$$L_e = L + \frac{b}{2} \left( \frac{r_c}{r_w} \right)^2.$$

When the first two terms on the lhs of Eq. (9) are zero, this condition reduces to Eq. (6) of Hyder et al. (1994).

Due to the presence of a second-order time derivative in Eq. (9), an additional initial condition

$$\frac{dH}{dt} \bigg|_{t=0} = H'_0, \quad (10)$$

is required, where  $H'_0$  is the initial velocity of water level movement as a result of slug-test initiation.

### 3. Solution

The features of the solutions presented here that set the apart from the solution of Hyder et al. (1994) are

1. Inclusion of wellbore inertial effects to model oscillatory responses; and
2. Use of the linearized kinematic condition at the water table.

To solve the flow problem, Eq. (9) is first rewritten in dimensionless form as

$$\beta_2 \frac{d^2 \Phi_{uc}}{dt_D^2} + \beta_1 \frac{d\Phi_{uc}}{dt_D} + \Phi_{uc} = \frac{1}{b_D} \int_{d_D}^{l_D} s_{D,1}(r_{D,w}, z_D, t_D) dz_D, \quad (11)$$

where  $\Phi_{uc} = H/H_0$  is the normalized source well response,  $s_{D,1} = s_1/H_0$  is the normalized skin response,  $t_D = t/T_c$ ,  $z_D = z/B$ ,  $r_{D,w} = r_w/B$  are dimensionless time and space coordinates,  $\beta_1 = 8\nu L/(r_c^2 g T_c)$ ,  $\beta_2 = L_e/(g T_c^2)$ ,  $T_c = B^2/\alpha_{r,1}$  is a characteristic time, and  $b_D = b/B$ ,  $d_D = d/B$ , and  $l_D = l/B$  are dimensionless test-configuration lengths and depths. For a complete list of dimensionless variables, see Table 1. Applying the Laplace transform to Eq. (11), with  $\Phi_{uc}(0) = 1$  and  $\Phi'_{uc}(0) = 0$ , leads to

$$\bar{\Phi}_{uc}(p) = \frac{\bar{f}(p)}{1 + p\bar{f}(p)}, \quad (12)$$

where  $p$  is the Laplace transform parameter,

$$\bar{f}(p) = \beta_1 + \beta_2 p + \gamma \bar{\Omega}/2, \quad (13)$$

$\gamma = K_{r,2}/K_{r,1}$ , and  $\bar{\Phi}_{uc}(p)$  is the Laplace transform of  $\Phi_{uc}(t_D)$ . The form of the function  $\bar{\Omega}$  is determined, in addition to the initial and boundary conditions already discussed above, by the choice of the boundary condition at the water table. In the following we give the form of this function for the case of (a) a constant head boundary condition, and (b) a moving water table condition approximated by the linearized kinematic condition used by Neuman (1972).

#### 3.1. Constant head boundary condition at water table

Hyder et al. (1994) used a constant head boundary condition at the water table in the KGS solution. This was felt justified because slug tests typically induce negligible water table displacements (Bouwer and Rice, 1976), especially if they are conducted more than a foot (0.3 m) below the water table. With this assumption, the flow problem is solved subject to

**Table 1**  
Dimensionless variables and parameters.

|  |
|--|
| $s_{D,i} = s_i/H_0$                    |
| $\Phi_{uc} = H(t)/H_0$                 |
| $r_D = r/B$                            |
| $r_{D,w} = r_w/B$                      |
| $r_{D,c} = r_c/B$                      |
| $r_{D,s} = r_s/B$                      |
| $z_D = z/B$                            |
| $d_D = d/B$                            |
| $l_D = \alpha_{r,1} t/B^2$             |
| $C_D = r_{D,c}^2/(b S_s)$              |
| $\alpha_D = \kappa \sigma$             |
| $\beta_1 = 8\nu L/(r_c^2 g T_c)$       |
| $\beta_2 = L_e/(g T_c^2)$              |
| $\beta_D = \beta_1/\sqrt{\beta_2}$     |
| $\kappa_i = K_{z,i}/K_{r,i}$           |
| $\sigma = B S_s/S_y$                   |
| $\gamma = K_{r,2}/K_{r,1}$             |
| $\beta = 1/b_D$                        |
| $\beta_D = \beta_1/\sqrt{\beta_2}$     |
| $\vartheta = 2b S_{s,2}(r_w/r_c)^2$    |
| $\zeta = d/b$                          |
| $\zeta_{sk} = r_{sk}/r_w$              |
| $\zeta_w = r_{D,w}\sqrt{\beta}$        |
| $\eta^2 = (p + a^2)/\kappa$            |
| $\psi_i = r_w/b\sqrt{K_{z,i}/K_{r,i}}$ |
| $\lambda = S_{s,2}/S_{s,1}$            |
| $R_1 = \gamma\vartheta/(2\lambda)$     |
| $R_2 = \vartheta/2$                    |

$$s_i(r, z = 0, t) = 0, \quad (14)$$

which corresponds to a constant head (no displacement) condition at the water table. The function  $\bar{\Omega}(r_{D,w}, p)$ , as determined by Hyder et al. (1994), is given by

$$\bar{\Omega}(r_{D,w}, p) = \sum_{n=1}^{\infty} g(n) \sin^2 \left( \frac{n\pi}{4\beta} \right) \sin^2 \left[ \frac{n\pi(1+2\zeta)}{4\beta} \right]. \quad (15)$$

where  $\beta = 1/b_D$ ,  $\zeta = d/b$ ,

$$g(n) = \beta \left( \frac{4}{n\pi} \right)^2 [1 + (-1)^{n+1} f_1(n)], \quad n = 1, 2, \dots, \quad (16)$$

$$f_1(n) = \frac{\chi_2 K_0(v_1) - \chi_1 I_0(v_1)}{v_1 [\chi_2 K_1(v_1) + \chi_1 I_1(v_1)]}.$$

$I_n()$  and  $K_n()$  are  $n$ -order modified Bessel functions of the first and second kinds, respectively. The details of the derivation of the KGS solution can be found in Hyder et al. (1994). The definitions of the variables and parameters are repeated here for completeness:

$$\chi_1 = K_0(v_1 \zeta_{sk}) K_1(v_2 \zeta_{sk}) - \left( \frac{N}{\gamma} \right) K_0(v_2 \zeta_{sk}) K_1(v_1 \zeta_{sk}),$$

$$\chi_2 = I_0(v_1 \zeta_{sk}) K_1(v_2 \zeta_{sk}) + \left( \frac{N}{\gamma} \right) K_0(v_2 \zeta_{sk}) I_1(v_1 \zeta_{sk}),$$

where the following quantities are only used in the KGS solution,  $N = v_1/v_2$ ,  $\zeta_{sk} = r_{sk}/r_w$ ,  $v_i = (\psi_i^2 \omega^2 + R_i p)^{1/2}$ ,  $\psi_i = (r_w/b) \sqrt{K_{zi}/K_{ri}}$ ,  $i = 1, 2$ ,  $\omega = (n - \frac{1}{2})\pi/\beta$ ,  $R_1 = \gamma\vartheta/(2\lambda)$ ,  $R_2 = \vartheta/2$ ,  $\lambda = S_{s,2}/S_{s,1}$ , and  $\vartheta = 2r_w^2 b S_{s,2}/r_c^2$ . Note that to extend the KGS solution to include inertial effects, and thus model oscillatory responses, one simply substitutes the function  $\bar{\Omega}(r_{D,w}, p)$ , derived by Hyder et al. (1994), into Eqs. (12) and (13). This solution is referred to, in this work, as the *unified* solution or model.

### 3.2. Linearized kinematic boundary condition at water table

For cases where the use of a constant head boundary condition at the water table is not justified, one may use the linearized kinematic boundary condition of Neuman (1972). The derivation is restricted to the case where wellbore skin effects can be neglected. In this case, the non-dimensional form of the boundary condition at the water table is

$$\left. \frac{\partial s_D}{\partial z_D} \right|_{z_D=0} = -\frac{1}{\alpha_D} \left. \frac{\partial s_D}{\partial t_D} \right|_{z_D=0}, \quad (17)$$

where  $s_D$  is the normalized aquifer response,  $\alpha_D = \kappa\sigma$ ,  $\kappa = K_z/K_r$ ,  $\sigma = BS_s/S_y$ , and  $S_y$  is specific yield. The subscript  $i$  is dropped here since effects of skin are not considered. We solve the flow problem described above using Laplace and Hankel transforms. It can be shown (see Appendix A for details) that

$$\bar{\Omega}(r_{D,w}, p) = \mathcal{H}_0^{-1} \{ \hat{\bar{\Omega}}(a, p) \} |_{r_{D,w}}, \quad (18)$$

where  $\mathcal{H}_0^{-1} \{ \}$  is the inverse zeroth-order Hankel transform operator,

$$\hat{\bar{\Omega}}(a, p) = \frac{C_D [1 - \langle \hat{w}_D(a, p) \rangle]}{\kappa \eta^2 \xi_w K_1(\xi_w)}, \quad (19)$$

$a$  is the Hankel transform parameter,  $C_D = r_{Dc}^2/(bS_s)$  is the dimensionless wellbore storage parameter,  $\eta^2 = (p + a^2)/\kappa$ ,  $\xi_w = r_{D,w}\sqrt{p}$ , and the function  $\langle \hat{w}_D \rangle$  is defined in Eq. (A.29) in Appendix A. Note that  $\gamma \equiv 1$  in this case, since we neglect skin effects. This solution is hereafter referred to as the moving water table (MWT) solution.

## 4. Model predicted behavior and validation

The solutions presented above are in Laplace–Hankel transform space. Inversion of the Laplace transforms was achieved numerically using the method of de Hoog et al. (1982). The code for the unified model was implemented in MATLAB, where the optimization toolbox was used to estimate parameters by nonlinear least squares. The MWT model code was written in FORTRAN where PEST (Doherty, 2002) is used to estimate hydraulic parameters. The codes are available upon request.

### 4.1. Response predicted with the unified solution

Eq. (12) is the unified solution to the slug test problem in unconfined aquifers that accounts for partial penetration, wellbore storage and finite wellbore skin with storage and hydraulic anisotropy. It can be used to model the entire range of responses (from underdamped to overdamped) that are typically observed in field slug tests. Fig. 2 shows the normalized response of the source well plotted against the dimensionless time  $t_D/\sqrt{\beta_2} = t\sqrt{g/L_e}$ , for different values of the parameter  $\beta_D = \beta_1/\sqrt{\beta_2}$ . The parameter  $\beta_D$  allows for the inertial effects given by the parameters  $\beta_1$  and  $\beta_2$  to be lumped into a single parameter, the effect of which can be presented in a single plot. The figure shows the whole range of head responses in the source well, from underdamped and highly oscillatory (small values of  $\beta_D$ ) to overdamped and monotonic, with increasing values of  $\beta_D$ .

Fig. 3 shows the model predicted response at different depths from the water table to the top of the test interval ( $d_D = d/B$ ) and for different lengths of the test interval ( $b_D = b/B$ ) in an aquifer with fixed hydraulic properties. The physical parameters used to compute the results are similar to those for BHRS tests, with  $K_{r,2} = 5.2 \times 10^{-3} \text{ m s}^{-1}$ ,  $K_{r,1} = 2 \times 10^{-4} \text{ m s}^{-1}$ ,  $r_w = 0.05 \text{ m}$ ,  $r_s = 0.06 \text{ m}$ ,  $r_c = 0.02 \text{ m}$ , and  $B = 20 \text{ m}$ . The results in Fig. 3a were obtained with  $b_D = 1.25 \times 10^{-2}$  and those in (b) with  $b_D = 2.5 \times 10^{-2}$ . The results shown in both (a) and (b) indicate that the predicted response becomes increasingly oscillatory with increasing depth. Additionally, comparing the responses in (a) to those in (b) indicates that the oscillations increase with increasing size of the test interval. For the overdamped responses, the decay to zero occurs more rapidly the longer the test interval length. The implication of these results is that a system that displays underdamped or critically damped responses near the water table may produce significantly oscillatory responses at greater depth or when the test interval length

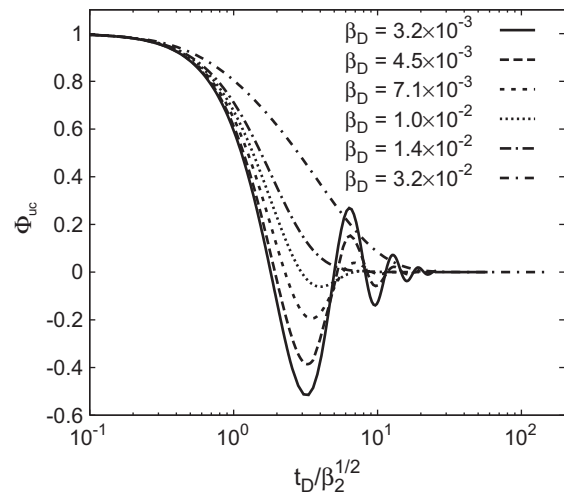
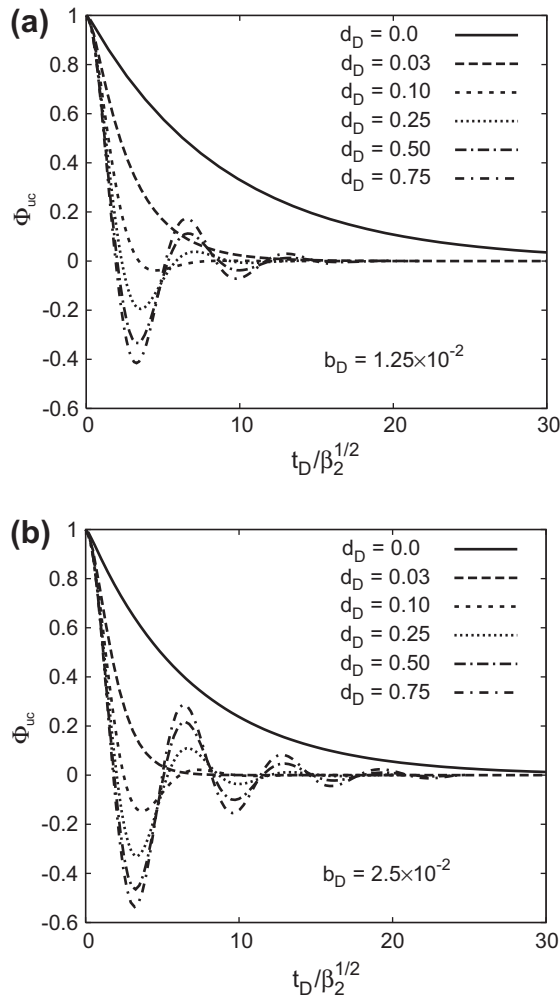


Fig. 2. Semi-log plot of dimensionless head,  $\Phi_{uc}(t_D)$ , computed with the unified model, against dimensionless time,  $t_D/\sqrt{\beta_2}$ , for different values of the dimensionless inertia parameter  $\beta_D$ . Oscillations diminish with increasing  $\beta_D$ .



**Fig. 3.** Linear plots of dimensionless head,  $\Phi_{uc}(t_D)$ , computed with the unified model, against dimensionless time,  $t_D/\sqrt{\beta_2}$ , for different values of the normalized depth below the water table,  $d_D$ , with a normalized test interval length of (a)  $b_D = 1.25 \times 10^{-2}$  and (b)  $b_D = 2.5 \times 10^{-2}$ .

is increased – all other factors being constant. This is due to the greater inertia within the wellbore at greater test depths, caused by a longer in-well water column.

#### 4.2. Response predicted with the MWT solution

The responses predicted by the MWT solution are shown in Fig. 4. The figure shows the effect of the dimensionless parameter  $\alpha_D = \kappa/\sigma$  on the response for (a) monotonic ( $\beta_D = 2.3 \times 10^{-4}$ ) and (b) oscillatory ( $\beta_D = 1.0 \times 10^{-3}$ ) behaviors. The results shown were computed with fixed  $\kappa = 10$  while the dimensionless storage parameter  $\sigma$  was varied. The parameter  $\sigma$  reflects the effect of the water table, with the confined condition corresponding to  $\sigma \equiv 0$ . The results indicate that there is appreciable sensitivity to  $\sigma$ , and therefore to water table displacement during the test. This is especially the case for monotonic responses that typically occur close to the water table. As one would expect, the effect of the water table diminishes with depth from the water table, as indicated by the oscillatory results shown in Fig. 4b, where the effect of the parameter  $\sigma$  is less than in the monotonic case (Fig. 4a).

The effect of the water table on the response with depth is shown in Fig. 5. Responses predicted by the MWT model at different depths below the water table,  $d_D$ , are compared to corresponding confined (BZ) and unified model responses. Compared to the BZ model (Fig. 5a), the largest effect is clearly for  $d_D = 0.0$ , the case where the

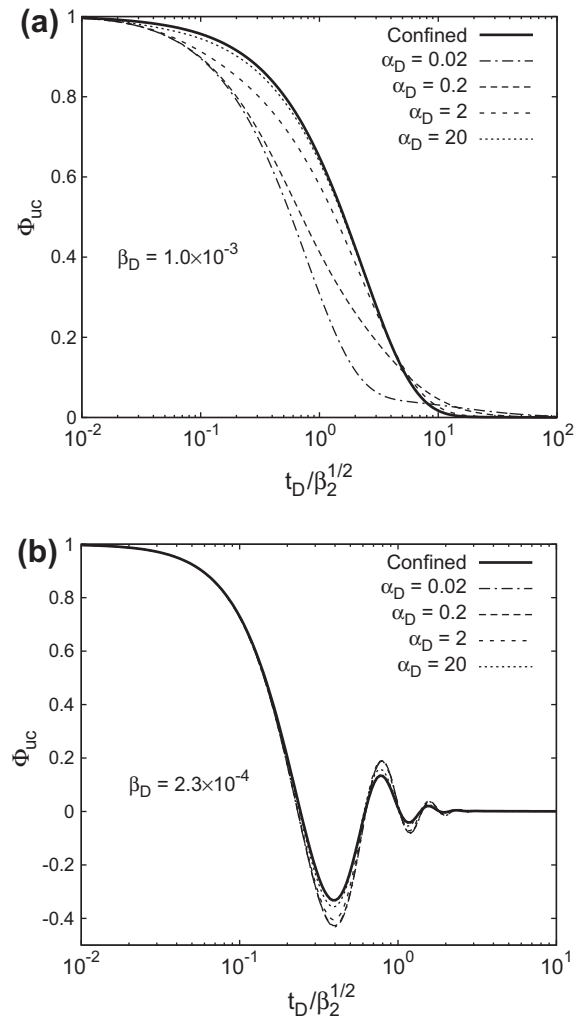


**Fig. 4.** Semi-log plots of dimensionless head,  $\Phi_{uc}(t_D)$ , computed with the kinematic water table boundary condition, against dimensionless time,  $t_D/\sqrt{\beta_2}$ , for different values of the dimensionless parameter  $\alpha_D = \kappa/\sigma$ , for (a) monotonic and (b) oscillatory responses.

top of the test interval is at the water table, but this effect diminishes rapidly with depth (see the minor effect at  $d_D = 0.05$ ). At a depth half way to the bottom of the aquifer ( $d_D = 0.5$ ), the responses of the two models are indistinguishable; the MWT response effectively behaves as if it were that of a confined formation. This suggests that one may use the confined aquifer BZ model to analyze unconfined aquifer slug test data with little error except at or very close to the water table ( $d_D < 0.05$ ).

In comparing the MWT solution to the unified model, shown in Fig. 5b, the two models do not converge with depth and the difference between the two responses does not appear to diminish with depth. This has the effect that the unified solution yields  $K$ -estimates that are systematically lower than those estimated with the MWT model. That these two models do not approach each other with depth should be clear from the boundary conditions used at the water table. Whereas setting  $S_y = 0$  in the MWT model yields the BZ solution, there are no limiting cases for which the boundary condition given in Eq. (17) becomes that given in Eq. (14).

#### 4.3. Validation of the models using field data from the MSEA Nebraska site

In this section we validate the unified and MWT models developed above by comparing the parameter estimates and



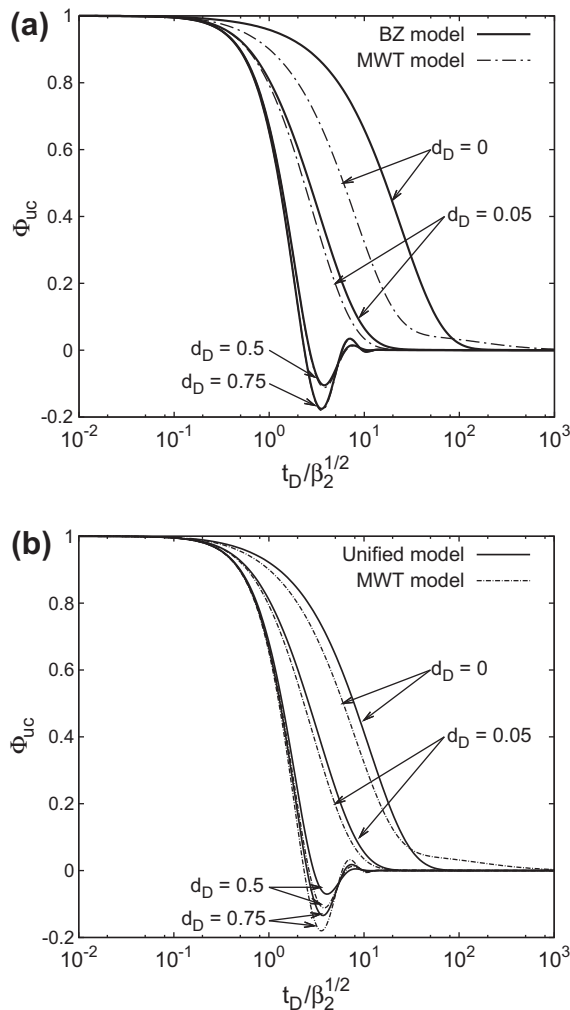


**Fig. 5.** Semi-log plots of dimensionless head,  $\Phi_{uc}(t_D)$ , against dimensionless time,  $t_D/\sqrt{\beta_2}$ , for different depths ( $d_D$ ) below the water table, comparing the MWT solution to (a) the confined aquifer (BZ) solution of Butler and Zhan (2004) and (b) the unified model.

model fits these two models yield to those obtained with other published methods. To achieve this objective, we use published slug test data collected with a straddle packer system in an unconfined fluvial sand and gravel aquifer at the MSEA site in Nebraska (McGuire, 1994; Zlotnik and McGuire, 1998). Details of the drilling and well installation procedures at the site can be found in McGuire (1994) and Zlotnik and McGuire (1998). The analysis presented here is based on the assumption that skin effects at the site can be neglected. The models are used to analyze slug test responses exhibiting both overdamped and underdamped responses.

The results of the inversion procedure using the SG (Springer and Gelhar, 1991) and KGS (Hyder et al., 1994) models, as well as the unified and MWT solutions, are shown in Fig. 6 and Table 3. Fig. 6a shows the overdamped case, whereas the oscillatory case is shown in Fig. 6b. As can be seen from the figure and the table, results obtained with the unified and MWT solutions are very similar to those obtained with the SG and the KGS models, as well as with the modified Springer–Gelhar method (ZM) of Zlotnik and McGuire (1998). The unified model admits estimation of all three parameters, namely,  $K$ ,  $S_s$  and  $L_e$ . The models of Springer and Gelhar (1991) and Zlotnik and McGuire (1998) do not account for formation elastic storage, whereas the KGS model does not apply to oscillatory responses. It should be recognized that estimating all three parameters simultaneously from slug test data is very difficult.

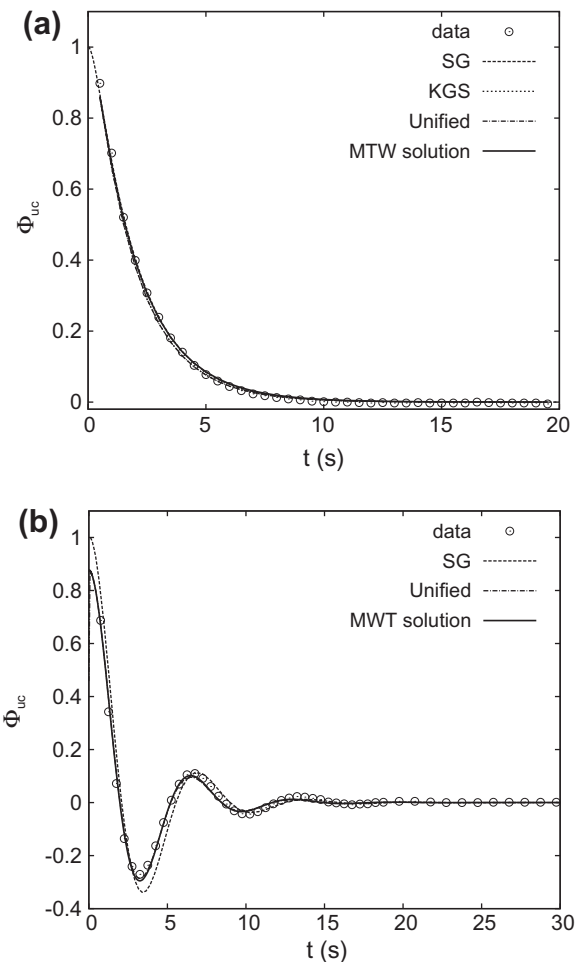


**Fig. 6.** Linear plots of model validation results. The unified and KGS solutions are fitted to field data and compared to the fits of existing models (data after McGuire (1994), Zlotnik and McGuire (1998)).

The advantage of the new model is that, where the specific storage is known (determined by other methods), it models the physics of flow associated with slug tests in unconfined aquifers more realistically than the SG model.

Additionally, the MWT solution admits specific yield, which governs the effects of the water table. Where slug tests are performed close to the water table, this should be the model of choice, provided the effects of wellbore skin are negligible. Since the BHRS data analyzed in this work were collected in wells known to show significant skin effects (Barrash et al., 2006), only the unified solution is discussed in the examples presented hereafter. A summary of slug test models and their applicability is given in Table 2.

#### 4.4. Comparison with Springer–Gelhar (SG) model

The SG model is widely used for estimating hydraulic conductivity in highly conductive unconfined aquifers. The model can be used to analyze the whole range of responses, from highly oscillatory to overdamped. The model cannot, however, be used to estimate specific storage or account for skin effects. In this section, we compare the hydraulic conductivity estimates obtainable with the SG model to the actual value used to simulate a slug test using the unified model developed herein. To accomplish this, simulated slug test responses were generated with the unified model using the fixed parameters  $B = 16.5$  m,  $b = 0.3$  m,  $K_{r,1} = K_{z,1} = 2 \times 10^{-4}$  m s<sup>-1</sup> (positive more permeable skin),  $S_{s,1} = 10^{-5}$  m<sup>-1</sup>,  $K_{r,2} = 5.2 \times$

**Table 2**  
Slug test models and their applicability.

| Model   | Oscillatory | Skin | Confined | Unconfined |
|---------|-------------|------|----------|------------|
| KGS     |             | X    | X        | X          |
| BZ      | X           | X    | X        |            |
| SG      | X           |      |          | X          |
| Unified | X           | X    |          | X          |
| MWT     | X           |      |          | X          |

**Table 3**  
Parameters estimated from the MSEA site slug test data.

| Model   | $K_{r,2} (\times 10^{-4} \text{ m s}^{-1})$ |         | $S_{s,2} (\times 10^{-5} \text{ m}^{-1})$ |         | $L_e (\text{m})$ |         |
|---------|---|---------|---|---------|------------------|---------|
|         | Zone 4                                      | Zone 14 | Zone 4                                    | Zone 14 | Zone 4           | Zone 14 |
| SG      | 4.5   | 16.5    | –   | –       | 4.79             | 10.55   |
| ZM      | 5.1   | 15.9    | –   | –       | 5.55             | 10.55   |
| KGS     | 5.5   | –       | 5.0                                       | –       | –                | –       |
| Unified | 4.5   | 15.0    | 5.0                                       | 5.0     | 4.64             | 9.64    |
| MWT     | 4.3   | 15.0    | 5.0                                       | 5.0     | 4.64             | 9.64    |

$10^{-3} \text{ m s}^{-1}$ ,  $r_w = 0.05 \text{ m}$ ,  $r_c = 0.02 \text{ m}$  and  $r_{sk} = 0.06 \text{ m}$ . The parameters  $K_{z,2}$ ,  $S_{s,2}$  and  $d$  were varied to simulate several field and test scenarios.

The objective of the simulation was to determine how the estimates of  $K_{r,2}$  (denoted  $K_{r,2}^*$ ) obtained with the SG model compare with the fixed value of  $K_{r,2} = 5.2 \times 10^{-3} \text{ m s}^{-1}$  used to generate the simulated response. The simulated response uses positive skin to reflect BHRS field conditions. We investigate the effects that  $\kappa$ ,

$S_{s,2}$ , and  $d_D$  have on  $K_{r,2}^*$ . The results are summarized in Fig. 7 where the ratio  $K_{r,2}^*/K_{r,2}$  is plotted against the dimensionless parameter  $\psi = (r_w/b) \sqrt{K_{z,2}/K_{r,2}}$  for different values of the dimensionless parameter  $\alpha = 2bS_{s,2}(r_w/r_c)^2$ . In these simulations, the values of  $\psi$  were obtained by varying  $\kappa_2$  over five orders of magnitude, and those of  $\alpha$  were obtained by varying  $S_{s,2}$  over three orders of magnitude. The simulations were conducted at four different values of  $d_D$ , as is indicated in the figure.

The results indicate that using the SG model to estimate  $K_{r,2}$  in a well with positive skin underestimates the hydraulic conductivity of an isotropic (high  $\psi$ ) formation by as much as 80%. Estimated values of  $K_{r,2}$  are close to the actual value used to generate the data when vertical hydraulic conductivity is significantly smaller than the radial value. Under these conditions, flow is predominantly radial. The results indicate that when flow deviates significantly from the radial direction, as would happen under near-isotropic conditions with small test intervals ( $b = 0.3 \text{ m}$ ), the SG model can significantly underestimate  $K_{r,2}$ . The value estimated with the SG model is some average of the skin and formation hydraulic conductivities.

The estimated values show a more modest sensitivity to  $S_{s,2}$  (i.e. to the dimensionless parameter  $\alpha$ ) and to  $d_D$ . This is particularly the case for large values of  $\psi$  (near isotropic aquifer conditions), as can be seen in Fig. 7, where estimated values of  $K_{r,2}$  do not change with the dimensionless parameter  $\alpha$ . However, for small values of  $\psi$  (highly anisotropic), where  $K_{r,2}$  values estimated with the SG model compare favorably with the true value, the estimated value can change by as much as 30% for a change in  $\alpha$  of three orders of magnitude.

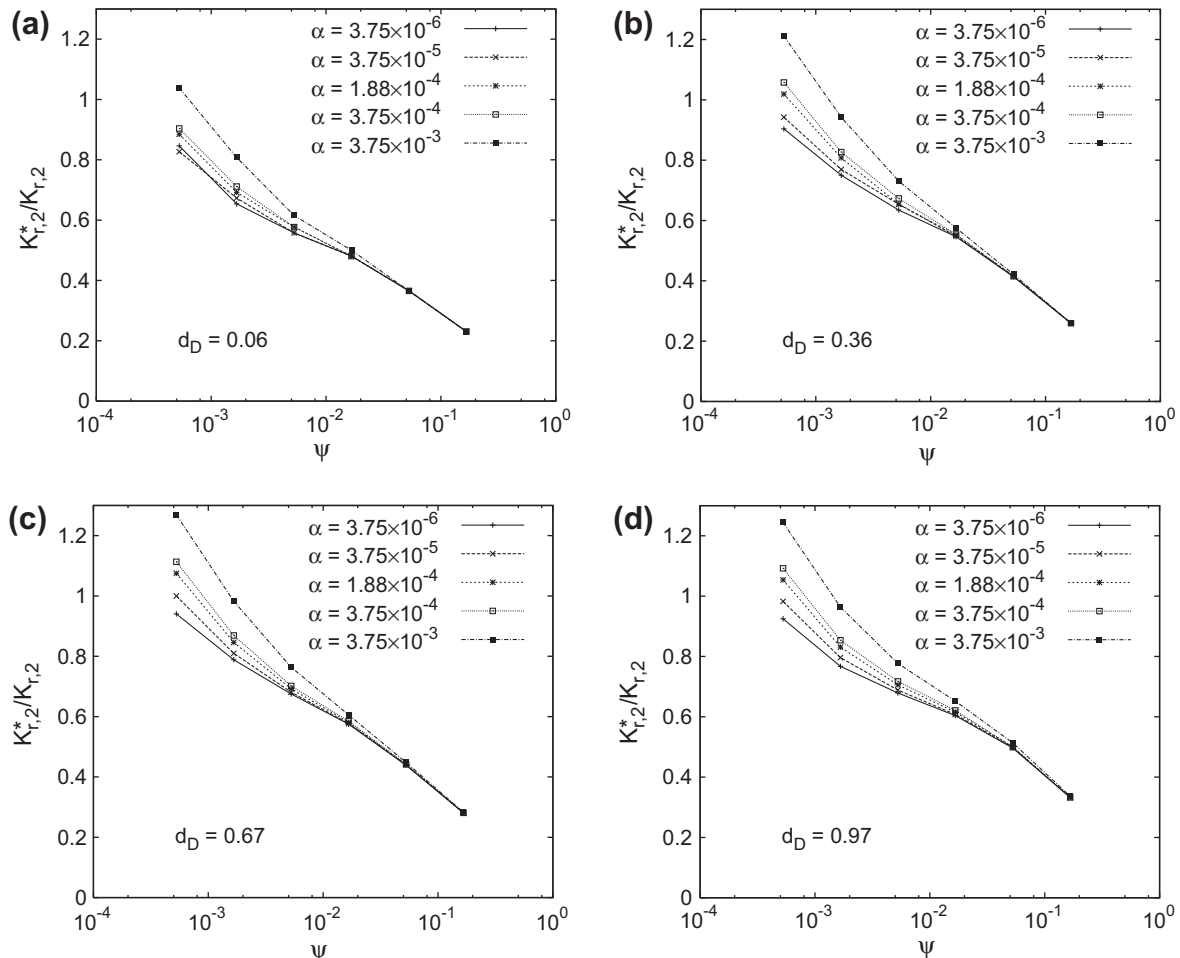


**Fig. 7.** Semi-log plot of  $K_{r,2}^*/K_{r,2}$  against the dimensionless parameter  $\psi = (r_w/b) \sqrt{K_{z,2}/K_{r,2}}$  for different values of the dimensionless parameter  $\alpha = 2bS_{s,2}(r_w/r_c)^2$ , at depths of (a)  $d_D = 0.06$ , (b)  $d_D = 0.36$ , (c)  $d_D = 0.67$  and (d)  $d_D = 0.97$ , to the top of the test interval.

#### 4.5. Comparison with Butler–Zhan (BZ) model

Due to the lack of a model that simulates oscillatory responses in unconfined aquifers in the manner of the confined BZ model, it is not uncommon for individuals to use the BZ model to analyze unconfined aquifer slug test data. Hence, in this section we investigate the conditions under which the unified model for unconfined aquifers predicts a response that coincides with that predicted by the confined aquifer BZ model (Butler and Zhan, 2004). Specifically, we compare results computed with the unified unconfined aquifer model to those computed with the BZ model for the same set of well and aquifer parameters. The models are compared at different  $d_D$  and for two different values of  $b_D$ . The results are shown in Fig. 8 where all the graphs labeled (a) were computed with  $b_D = 1.25 \times 10^{-2}$  and those labeled (b) were computed with  $b_D = 2.5 \times 10^{-2}$ .

The results in Fig. 8 show that for a small test interval ( $b_D = 1.25 \times 10^{-2}$ ), the two models give significantly different results at almost all depths, except very close to the base of the aquifer where a no-flow boundary condition is used in both models. Hence, using the BZ model to estimate hydraulic parameters of an unconfined aquifer would yield erroneous results at almost all depths if the test interval is small relative to the thickness of the

formation. However the differences between the two models appear small when  $d_D$  is greater than 0.25 that were tested but are not shown here for brevity. This maybe due to the fact that for large values of  $b_D$  flow is predominantly radial. Hence, for relatively large values of  $b_D$ , and at sufficient depth from the water table, using the confined aquifer BZ model to estimate hydraulic parameters of an unconfined aquifer would yield reasonable values.

Fig. 9 shows the estimates obtained with the BZ model using simulated data generated with the unified unconfined aquifer model developed herein. In Fig. 9a  $K_{r,2}^*$  is normalized by the actual value of  $K_{r,2}$  used to generate the simulated data; this ratio is plotted against the dimensionless parameter  $\psi = (r_w/b) \sqrt{K_{z,2}/K_{r,2}}$ . In (b) the estimated specific storage,  $S_{s,2}^*$ , normalized by the actual value,  $S_{s,2}$ , is plotted against  $\psi$ . The results were obtained at  $d_D = 0.25$  using  $b_D = 1.25 \times 10^{-2}$  and  $b_D = 2.5 \times 10^{-2}$ . As discussed above, it can be clearly seen in these results that for the larger value of  $b_D$ , the BZ model yields estimates of hydraulic conductivity ( $K_{r,2}^*$ ) that are closer to the true value. For  $b_D = 1.25 \times 10^{-2}$ , the error committed when one uses the confined aquifer model to estimate unconfined aquifer hydraulic conductivity can be as large as 35% for highly anisotropic formations. A change in anisotropy by five orders of magnitude leads to only modest improvements in the estimated value. Doubling the length of the test interval to

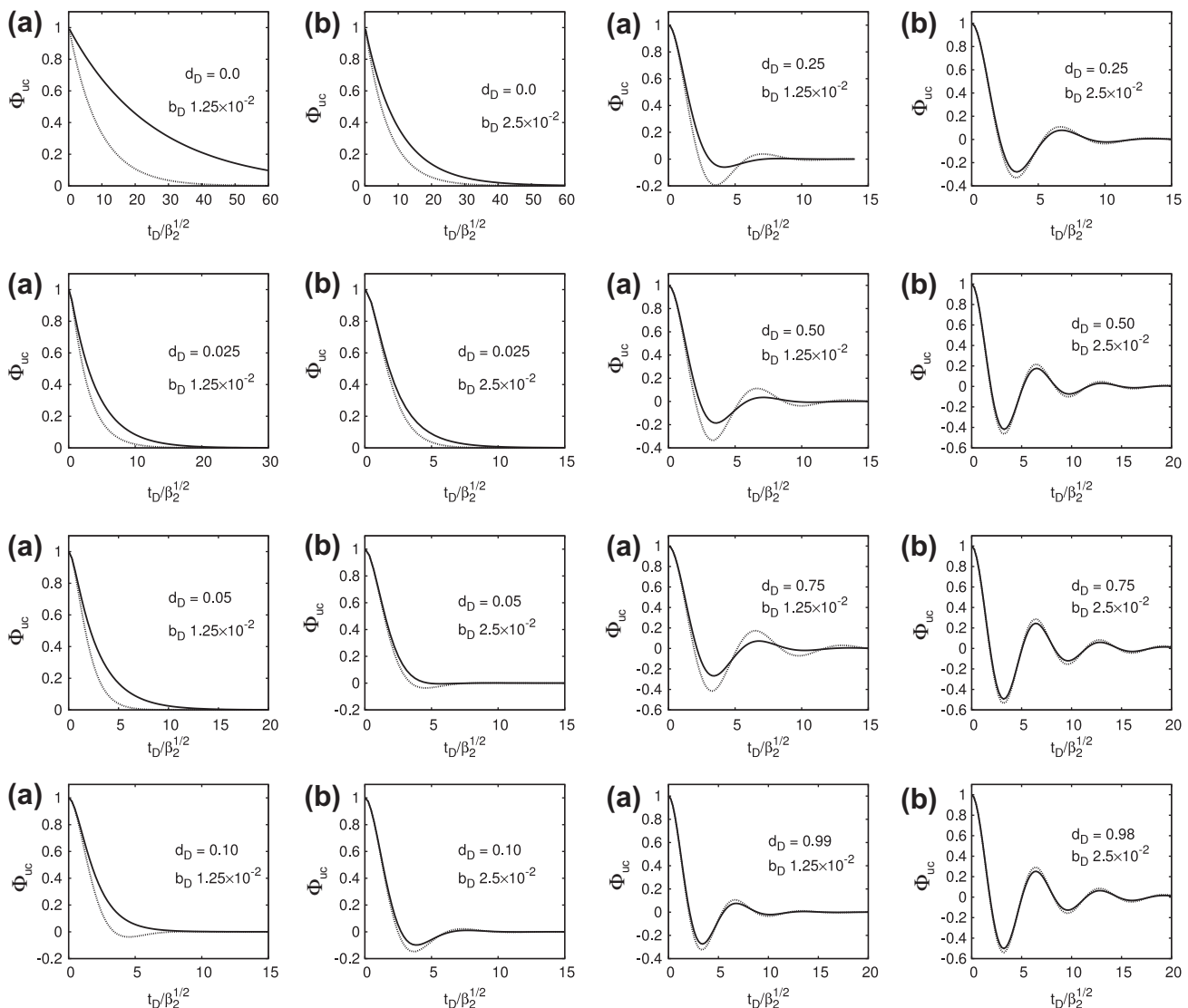
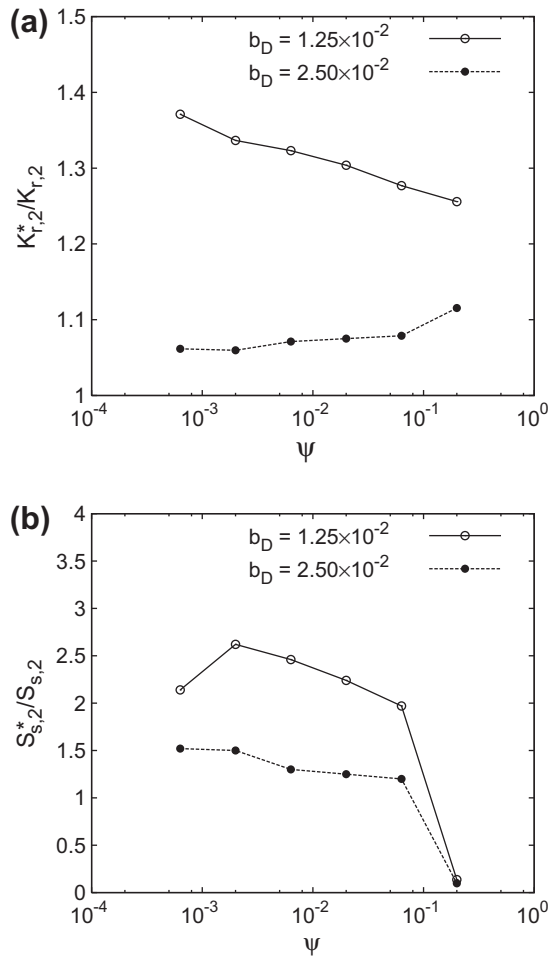


Fig. 8. Comparison of the unified unconfined aquifer model developed here (dotted line) with the model of Butler and Zhan (2004) (solid line) at the indicated normalized depths to test interval for (a)  $b_D = 1.25 \times 10^{-2}$  and (b)  $b_D = 2.5 \times 10^{-2}$ .





**Fig. 9.** Linear plots of (a)  $K_{r,2}^*/K_{r,2}$  and (b)  $S_{s,2}^*/S_{s,2}$  against the dimensionless parameter,  $\psi = (r_w/b)\sqrt{K_{z,2}/K_{r,2}}$ , for two different values of the dimensionless test interval length ( $b_D = 1.25 \times 10^{-2}$  and  $b_D = 2.5 \times 10^{-2}$ ), at  $d_D = 0.25$ .

$b_D = 2.5 \times 10^{-2}$  significantly improves the estimate of hydraulic conductivity. For this value of  $b_D$ , the largest error committed by using the confined aquifer model is around 10%. Estimates of specific storage show similar sensitivity to the size of the test interval, though the errors committed are significantly larger ( $\sim 100\%$ ).

## 5. Model application to slug test data from the BHRS

The aquifer at the Boise Hydrogeophysical Research Site (BHRS) near Boise, Idaho, is an unconfined fluvial aquifer consisting largely of cobbles and sand (Barrash and Reboulet, 2004). Slug tests were conducted in the aquifer at the BHRS in 2008 and 2009 in wells that were drilled with the core-drill-drive method and completed with 10-cm inner diameter PVC slotted casing. The wells show evidence of positive wellbore skin that has been attributed to partial sand invasion of screen slots (Barrash et al., 2006). The test intervals were isolated with a straddle packer and three tests were conducted in each interval to ensure repeatability of the experimental results. Similar results were obtained in each interval for all three tests. Test data are used as examples from BHRS well B5 for intervals with overdamped behavior (upper at 8.69–8.99 m below measuring point (BMP)) and underdamped behavior (lower at 10.21–10.51 m BMP).

In this parameter estimation exercise,  $S_{s,1} = S_{s,2} = 5 \times 10^{-5} \text{ m}^{-1}$ , based on findings at the BHRS from fully penetrating pumping tests (Fox, 2006; Barrash et al., 2006) and on published findings for other

unconsolidated sandy fluvial aquifers (Bohling et al., 2007; Moench et al., 2001). Additionally,  $\kappa_1 = \kappa_2 = 1$ . The data are analyzed for scenarios with and without skin to provide some insight on the sensitivity of formation parameters to skin properties.

For solutions that include skin, and especially positive skin (i.e., BHRS cases below), it is recognized that it is difficult to estimate both aquifer and skin conductivity simultaneously, because they act in series and hence are highly (negatively) correlated. Initial estimates for  $K_{r,1}$  and  $K_{r,2}$  were taken from analytical solutions of fully penetrating pumping test data at the BHRS (Fox, 2006; Barrash et al., 2006). However, reasonable parameter estimates were difficult to obtain from the slug test data using the value  $K_{r,1} = 2 \times 10^{-5} \text{ m s}^{-1}$ , obtained from fully penetrating pumping tests. We used the value  $K_{r,1} = 2 \times 10^{-4} \text{ m s}^{-1}$  in modeling the BHRS slug tests; this value was determined by trial-and-error to be the lowest consistent value giving reasonable results. Comparable (same order of magnitude) results for  $K_{r,1}$  have been obtained by inversion of the BHRS slug test data (Cardiff et al., 2011).

Fig. 10 shows the results of the model fit for the overdamped response recorded in the upper B5 test interval, and the oscillatory response in lower B5 test interval. The parameter values obtained with the unified solution are summarized in Table 4. For the overdamped case, the results are very similar to those with the KGS method of Hyder et al. (1994). However, the unified solution is the only analytical solution that can treat slug tests with oscillatory

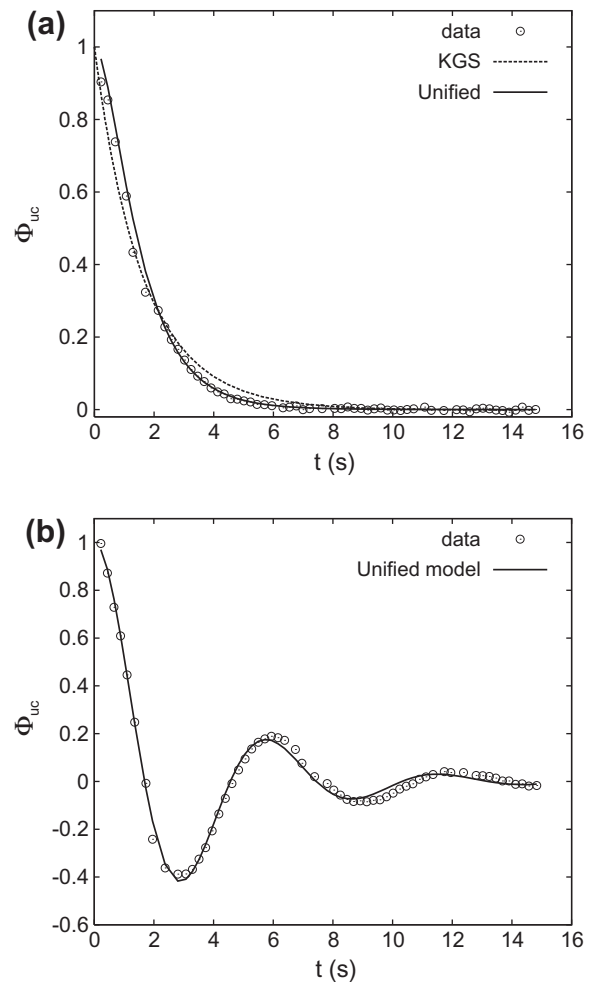


**Fig. 10.** Linear plots of model fit to BHRS B5 slug test data in test intervals (a) 8.69–8.99 m (overdamped) and (b) 10.21–10.51 m (oscillatory) below the measuring point;  $K_{r,1} = 2.0 \times 10^{-4} \text{ m s}^{-1}$ .

**Table 4**

Parameters estimated from slug test data obtained at the BHRS in well B5. The parameter pairs correspond, respectively, to the test intervals 8.69–8.99 m (zone 1, overdamped) and 10.21–10.51 m (zone 2, oscillatory) below the measuring point.

| Model   | $K_{r,2}$<br>( $\times 10^{-4} \text{ m s}^{-1}$ ) |        | $S_{s,2}$<br>( $\times 10^{-5} \text{ m}^{-1}$ ) |        | $L_e$ (m) |        | $K_{r,1}$<br>( $\times 10^{-4} \text{ m s}^{-1}$ ) |        |
|---------|--|--------|--|--------|-----------|--------|--|--------|
|         | Zone 1   | Zone 2 | Zone 1   | Zone 2 | Zone 1    | Zone 2 | Zone 1   | Zone 2 |
| KGS     | 7.5  | –      | 5.0  | –      | –         | –      | 2.3  | –      |
| unified | 6.8  | 55.3   | 5.0  | 5.0    | 6.45      | 8.20   | 2.0  | 2.0    |
| SG      | 4.8  | 18.0   | –  | –      | 6.31      | 8.23   | No skin  | –      |
| KGS     | 6.3  | –      | 5.0  | –      | –         | –      | No skin  | –      |
| unified | 5.8  | 20.0   | 5.0  | 5.0    | 6.45      | 8.20   | No skin  | –      |

behavior in unconfined aquifers with partially penetrating wells, wellbore skin, and aquifer and skin elastic storage.

## 6. Empirical sensitivity analysis

In this section we consider the sensitivity of the estimates of  $K_{r,2}$  to  $K_{r,1}$  and  $r_s$ . For the results presented here,  $\kappa_1 = \kappa_2 = 1$ , and  $S_{s,1} = S_{s,2} = 5 \times 10^{-5} \text{ m}^{-1}$ ;  $r_w = 0.051 \text{ m}$ . The data from the overdamped example in well B5 at the BHRS were used to estimate formation hydraulic conductivity for different values of skin hydraulic conductivity and radial extent.

In the first instance, the model fits are shown in Fig. 11, and the parameter values are listed in Table 4. Skin hydraulic conductivity is forced to be equal to that of the formation to simulate the case without wellbore skin. For this case hydraulic estimates were found to be 10–15% lower than those obtained above with positive wellbore skin for the overdamped case. The model was found to fit the data as well as the fit obtained in the case of positive skin. The parameter values obtained using the unified solution are very similar to those obtained with the SG and KGS models. For the underdamped case without skin, estimated hydraulic conductivity values were found to be 60% lower than for the case with positive skin. The parameter values obtained with the unified model compare well to those obtained with the SG method.

Secondly,  $K_{r,1}$  and  $r_s$  are allowed to vary and we note their effect on estimates of hydraulic conductivity. The results are summarized in Table 5. They indicate that for a given value of  $r_s$ , the  $K_{r,2}^*$  increases with decreasing values of  $K_{r,1}$ . Additionally, for a given  $K_{r,1}$ , the  $K_{r,2}^*$  increases with increasing  $r_s$  if  $\gamma > 1$  (positive skin). Increasing  $r_s$  from 0.057 m to 0.087 m, then to 0.108 m, yielded progressive increases in estimated formation hydraulic conductivity by factors of about 3 and 150, respectively, for the positive skin case with  $K_{r,1} = 2 \times 10^{-4} \text{ m s}^{-1}$ . Further reduction of  $K_{r,1}$  by 50%, leads to convergence failure during the formation conductivity estimation exercise. For the case of negative skin (i.e.,  $\gamma < 1$ , as in a sand or gravel filter pack),  $K_{r,2}^*$  showed only moderate sensitivity to  $K_{r,1}$  and  $r_s$ . Nevertheless, as expected,  $K_{r,2}^*$  decreases with increasing  $r_s$ .

The estimability (identifiability) of specific yield,  $S_y$ , and anisotropy ratio,  $\kappa$ , from slug test data could be rigorously addressed by numerically or analytically computing the sensitivity of model predicted slug test response to these two parameters. It is also possible to qualitatively observe this sensitivity by plotting model-predicted responses for different values of the parameter  $S_y$  or  $\kappa$ , with all other parameters held constant. Fig. 12 shows this for  $S_y$  and Fig. 13 for  $\kappa$ . Although semi-log space curves in Fig. 12a are indistinguishable, the log–log space curves (Fig. 12b) are significantly dissimilar. This is also the case for variable  $\kappa$ ; the semi-log plot (Fig. 13a) shows much less variation than the log–log plot (Fig. 13b); the shapes of the log–log curves for different values of  $\kappa$  are appreciably dissimilar, indicating sensitivity of model pre-

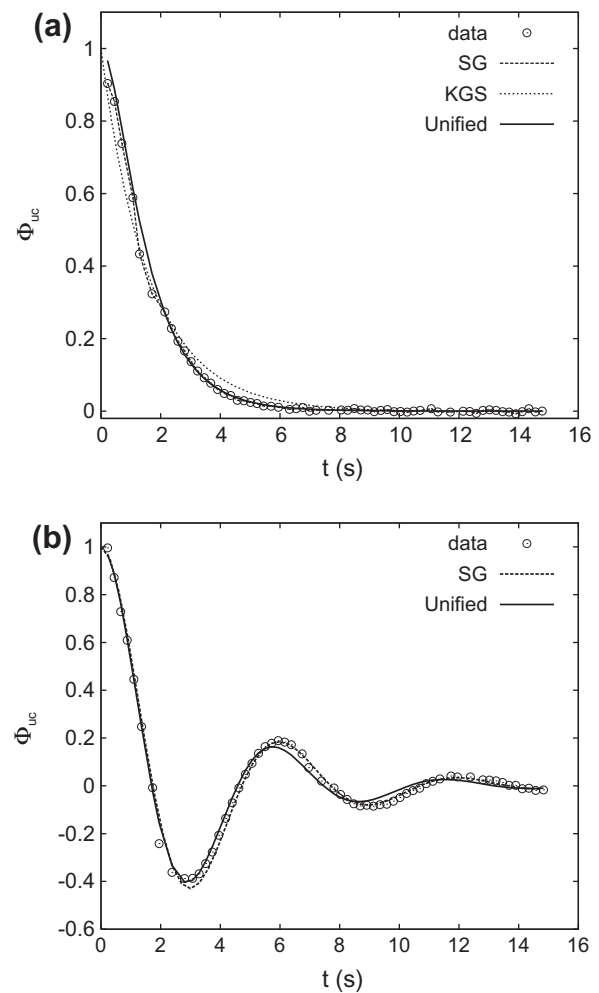


**Fig. 11.** Linear plots of model fit to BHRS B5 slug test data in test intervals (a) 8.69–8.99 m (overdamped) and (b) 10.21–10.51 m (oscillatory) below the measuring point, assuming no skin.

**Table 5**

Sensitivity of formation hydraulic conductivity to skin hydraulic conductivity and radial extent.

| $K_{r,1}$ ( $\times 10^{-4} \text{ m s}^{-1}$ ) | $K_{r,2}$ ( $\times 10^{-4} \text{ m s}^{-1}$ ) |                         |                         |
|---|---|-------------------------|-------------------------|
|   | $r_s = 0.057 \text{ m}$                         | $r_s = 0.087 \text{ m}$ | $r_s = 0.108 \text{ m}$ |
| 100   | 4.7   | 2.3                     | 1.6                     |
| 50  | 5.0   | 3.3                     | 2.3                     |
| 20  | 5.3   | 4.0                     | 3.3                     |
| 2   | 6.8   | 21.0                    | 1336                    |
| 1   | 8.5   | –                       | –                       |
| 0.5   | 18.0  | –                       | –                       |

dicted response to this parameter, particularly at late time and at small values of the normalized response.

Typical pressure transducers have a millimeter-scale sensitivity to water level changes, and slug test initial displacements are typically of the order of a few (5–25) cm. It is, therefore, a challenge to collect meaningful late-time data where model predicted sensitivity to  $S_y$  and  $\kappa$  is most pronounced. However, this may be mitigated by using large initial displacements, though this may introduce nonlinear inertial effects in the wellbore. Fig. 12c is a plot of data collected at a site near Butte, Montana, in the summer of 2010 that shows an inflection indicative of water-table and, possibly, anisotropy effects. The pneumatic slug tests were conducted with relatively large initial displacements (>50 cm), which induced lar-

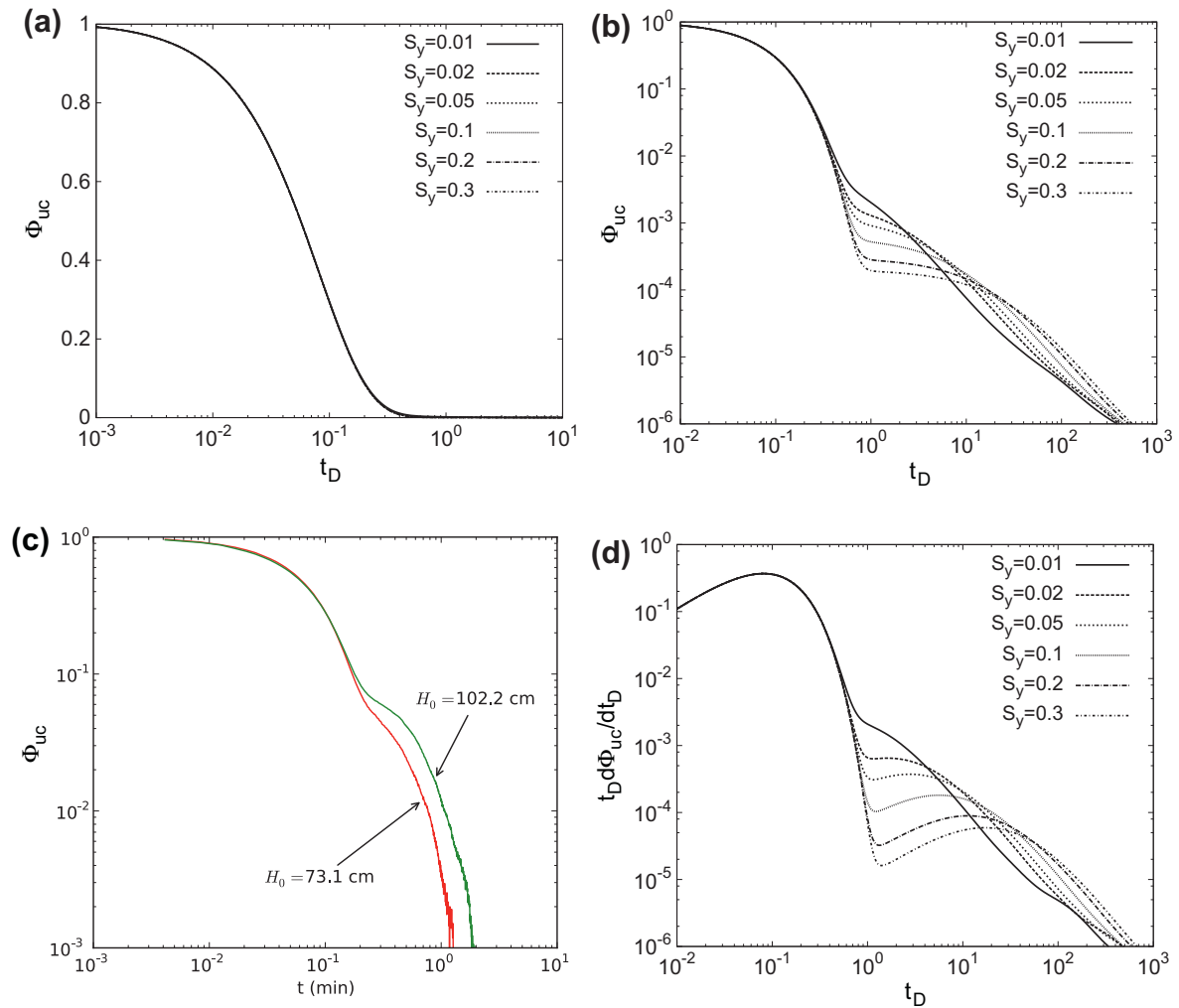


**Fig. 12.** Plots of dimensionless head,  $\Phi_{uc}(t_D)$ , computed with the kinematic boundary condition at the water table, against dimensionless time,  $t_D$ , on (a) semi-log and (b) log-log scale, for different values of specific yield,  $S_y$ , with  $\kappa = 1.0$  with  $d = 1.0$  m and  $l = 1.3$  m. The plot in (c) shows slug test data collected at a site near Butte, Montana, and (d) shows the log-time/derivative of the predicted response  $\partial\Phi_{uc}/\partial\ln(t_D)$ .

ger than typical volumes of water flow between the well and the aquifer with possible impact on water table position. The behavior under such flow conditions may be more correctly modeled with a

linearized kinematic condition than with a constant head at the water table. Work is presently under way to determine under what conditions  $S_y$  and the  $\kappa$  are practically estimable from such data.

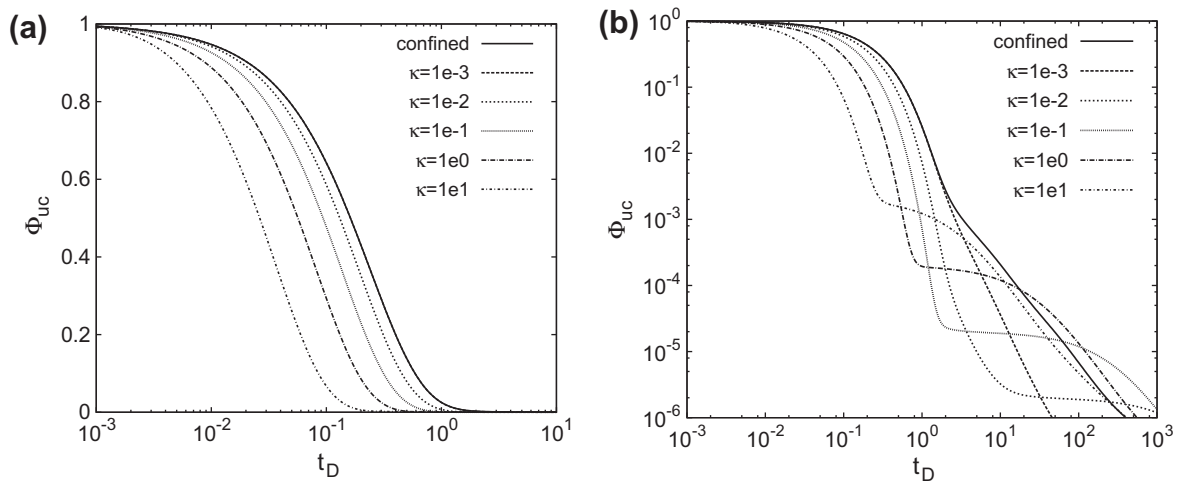


**Fig. 13.** Plots of dimensionless head,  $\Phi_{uc}(t_D)$ , computed with the kinematic boundary condition at the water table, against dimensionless time,  $t_D$ , on (a) semi-log and (b) log-log scale, for different values of the anisotropy ratio,  $\kappa$ , with  $S_y = 0.3$ , with  $d = 0.0$  m and  $l = 0.3$  m.

We also mention here in passing that the identifiability of  $S_y$  and  $\kappa$  from slug test data may be significantly enhanced by consideration of the first temporal derivative of slug test responses (see Fig. 12d), an approach that is outside the scope of this work but is being explored in current research efforts by the authors.

## 7. Discussion and conclusions

The unified and MWT solutions developed in this work can be used to model slug tests in unconfined aquifers for the whole spectrum of responses ranging from overdamped to highly oscillatory. The MWT solution is limited to wells where skin effects are negligible, but extension of the solution to include skin effects is a direction for further development. Results with the unified model give values of formation  $K$  that are systematically lower at all depths than those obtained with the MWT model, as seen in Fig. 5b. For published field data, the two models yield comparable parameter estimates. In principle one may use the MWT model to estimate specific yield from slug test data collected in unconfined aquifers. It has also been demonstrated in this work that the MWT solution becomes the confined aquifer solution of Butler and Zhan (2004) deep into the formation.

The unified model accounts for the effects of skin of finite radial extent. Skin and aquifer formation elastic storage and vertical anisotropy are also accounted for in this model. The model was validated by comparing the parameter estimates obtained with this model with published estimates obtained with other models. Specifically, the model validation exercise was based on field data from the MSEA Nebraska site and reported in McGuire (1994), and Zlotnik and McGuire (1998). The unified model yielded parameter estimates that compare well with those obtained with the SG (Springer and Gelhar, 1991), KGS (Hyder et al., 1994), ZM (Zlotnik and McGuire, 1998) and MWT models (see Table 4). The main advantage of the unified model over these other models is that it is the only model for unconfined aquifers that (a) admits all the three pertinent parameters, namely, hydraulic conductivity, specific storage and  $L_e$ , (b) can model overdamped and oscillatory responses, and (c) includes wellbore skin. The SG and ZM models do not account for formation elastic storage, whereas the KGS model does not apply to oscillatory responses (Table 2).

Additionally, the SG model was used to estimate the formation hydraulic conductivity associated with the system behavior simulated with the unified model. The objective was to determine under what conditions the two models yield similar parameter values. The estimated values were found to show significant sensitivity to formation anisotropy as encapsulated in the dimensionless parameter  $\psi$  for the case with positive wellbore skin. For the test configuration used in the simulation, it was found that the estimates obtained with the SG model compare well with the actual hydraulic conductivity value under conditions where radial flow is predominant (high  $K_{r,2}$  and low  $K_{z,2}$ ). The deviation from the true value was found to be as large as 80% under isotropic conditions. Even though these results were obtained for the case with  $K_{r,1} < K_{r,2}$  (positive skin) for generality, they can be extended to the case of no wellbore skin ( $K_{r,1} = K_{r,2}$ ), but with the expectation that smaller deviations of  $K_{r,2}^*$  from  $K_{r,2}$  would be observed.

The conditions under which one could use the confined aquifer BZ model to model the unconfined aquifer response were also investigated. The results obtained in this work indicate that if the test interval is small relative to the thickness of the formation, parameter values estimated with a confined aquifer model can be significantly overestimated irrespective of the depth at which the test was conducted. However, doubling the test interval length significantly improved the parameter estimates obtained with the confined aquifer model. These results seem to indicate that when

flow is predominantly radial, the BZ model compares well to the unified model developed herein. Nevertheless, caution has to be used where high-spatial-resolution slug tests are conducted in relatively short test intervals (e.g., in the range  $b \sim 20\text{--}30$  cm). Under such testing conditions one has to use the unified model developed herein to estimate formation hydraulic parameters.

It should be noted also that, because  $K_{r,1}$  and  $K_{r,2}$  act in series, it is difficult to estimate both simultaneously from single-well slug test data, even when the values for  $r_s$  and  $S_{s,1}$  are given. For the case of slug tests conducted in well B5 at the BHRS, the sensitivity of  $K_{r,2}$  to  $K_{r,1}$  was found to decrease with decreasing values of  $K_{r,1}$ . In fact, for  $K_{r,1} \leq 2 \times 10^{-5} \text{ m s}^{-1}$  the inversion does not yield a solution for  $K_{r,2}$  due to the very low sensitivity of  $K_{r,2}$  on these relatively low values of  $K_{r,1}$ . To obtain the  $K_{r,2}$  values reported herein, we set  $K_{r,1} = 2 \times 10^{-4} \text{ m s}^{-1}$ , which is about 10 times larger than values from the analytical modeling of fully penetrating pumping tests reported by Fox (2006) and Barrash et al. (2006). This led to formation hydraulic conductivity estimates that are about 1.2–3 times larger than thickness-averaged formation hydraulic conductivity values from previous works.

The unified model was also used to consider effects of varying magnitudes of negative skin. Results indicate that the estimated formation hydraulic conductivity can decrease by a factor of 2–3 to compensate for increases of negative skin hydraulic conductivity of an order of magnitude. Additionally, the relative effect of skin increases with increasing annular radial increment of skin. The impact, however, is much more significant for positive skin than negative skin.

Analysis of the MWT model responses to specific yield,  $S_y$ , and aquifer hydraulic anisotropy,  $\kappa$ , indicates that it may be possible to estimate these two parameters from slug test data. For the effects of the water table, as predicted by model with the linearized kinematic condition, to be observable in the data, one would need either (a) a large initial displacement, or (b) transducers with sub-millimeter sensitivity to water level fluctuations. These effects are only discernible when one plots the data on log–log scale or takes the log-scale temporal derivative of the data. Work is currently under way to attempt to estimate  $S_y$  and  $\kappa$  using the MWT model and data generated with large initial displacements.

## Acknowledgments

Support for this research was provided by NSF Grant EAR-0710949, EPA Grant X-96004601-0 and a grant from the Montana Water Center through the US Geological Survey Water Resources Research Program. We gratefully acknowledge helpful discussions and sharing of models with Geoff Bohling and Jim Butler, and discussions and sharing of data from slug tests in Nebraska by Vitaly Zlotnik, Virginia McGuire, and Brian Zurbuchen. Sandia National Laboratories is a multi-program laboratory managed and operated by Sandia Corporation, a wholly owned subsidiary of Lockheed Martin Corporation, for the US Department of Energy's National Nuclear Security Administration under contract DE-AC04-94AL85000.

## Appendix A. Solution with “moving” water table

The solution to this problem can be written in dimensionless form as

$$S_D = \begin{cases} s_D^{(1)} & \forall z_D \in [0, d_D] \\ s_D^{(2)} & \forall z_D \in [d_D, l_D] \\ s_D^{(3)} & \forall z_D \in [l_D, 1], \end{cases} \quad (\text{A.1})$$

where  $s_D^{(n)}$  solves

$$\frac{\partial s_D^{(n)}}{\partial t_D} = \frac{1}{r_D} \frac{\partial}{\partial r_D} \left( r_D \frac{\partial s_D^{(n)}}{\partial r_D} \right) + \kappa \frac{\partial^2 s_D^{(n)}}{\partial z_D^2}. \quad (\text{A.2})$$

The initial and boundary conditions are

$$s_D^{(n)} \Big|_{t_D=0} = s_D^{(n)} \Big|_{r \rightarrow \infty} = 0 \quad (\text{A.3})$$

$$\lim_{r_D \rightarrow 0} r_D \frac{\partial s_D^{(1)}}{\partial r_D} = \lim_{r_D \rightarrow 0} r_D \frac{\partial s_D^{(3)}}{\partial r_D} = 0 \quad (\text{A.4})$$

$$\frac{\partial s_D^{(1)}}{\partial z_D} \Big|_{z_D=0} = -\frac{1}{\alpha_D} \frac{\partial s_D^{(1)}}{\partial t_D} \Big|_{z_D=0} \quad (\text{A.5})$$

$$\frac{\partial s_D^{(3)}}{\partial z_D} \Big|_{z_D=1} = 0 \quad (\text{A.6})$$

$$r_D \frac{\partial s_D^{(2)}}{\partial r_D} \Big|_{r_D=r_{D,w}} = C_D \frac{d\Phi_{uc}}{dt_D}, \quad (\text{A.7})$$

$$\Phi_{uc}(t_D = 0) = 1.0, \quad (\text{A.8})$$

and

$$\beta_2 \frac{d^2 \Phi_{uc}}{dt_D^2} + \beta_1 \frac{d\Phi_{uc}}{dt_D} + \Phi_{uc} = \frac{1}{b_D} \int_{d_D}^{l_D} s_D^{(2)}(r_{D,w}, z_D, t_D) dz_D. \quad (\text{A.9})$$

Additionally, continuity of head and flux is imposed at  $z_D = d_D$  and  $z_D = l_D$  as follows:

$$s_D^{(1)} \Big|_{z_D=d_D} = s_D^{(2)} \Big|_{z_D=d_D}, \quad (\text{A.10})$$

$$\frac{\partial s_D^{(1)}}{\partial z_D} \Big|_{z_D=d_D} = \frac{\partial s_D^{(2)}}{\partial z_D} \Big|_{z_D=d_D}, \quad (\text{A.11})$$

$$s_D^{(3)} \Big|_{z_D=l_D} = s_D^{(2)} \Big|_{z_D=l_D}, \quad (\text{A.12})$$

and

$$\frac{\partial s_D^{(3)}}{\partial z_D} \Big|_{z_D=l_D} = \frac{\partial s_D^{(2)}}{\partial z_D} \Big|_{z_D=l_D}. \quad (\text{A.13})$$

This flow problem is solved using Laplace and Hankel transforms. Taking the Laplace and Hankel transforms of Eq. (A.2) for  $n = 1, 3$ , and taking into account the initial and boundary conditions in Eqs. (A.3) and (A.4), gives the ordinary differential equation

$$\frac{d^2 \hat{s}_D^{(n)}}{dz_D^2} - \eta^2 \hat{s}_D^{(n)} = 0 \quad (\text{A.14})$$

where  $\hat{s}_D^{(n)} = \mathcal{H}\{\mathcal{L}\{s_D^{(n)}\}\}$  is the double Laplace–Hankel transform of the function  $s_D^{(n)}$ ,  $\eta^2 = (p + a^2)/\kappa$ , and  $p$  and  $a$  are the Laplace and Hankel transform parameters, respectively. Eq. (A.14) has the general solution

$$\hat{s}_D^{(n)} = A_n e^{\eta z_D} + B_n e^{-\eta z_D}. \quad (\text{A.15})$$

The boundary condition at the water table, Eq. (A.15), in Laplace–Hankel transform space, becomes

$$\frac{d\hat{s}_D^{(1)}}{dz_D} \Big|_{z_D=0} = -\frac{p}{\alpha_D} \hat{s}_D^{(1)} \Big|_{z_D=0}. \quad (\text{A.16})$$

Applying this boundary condition leads to

$$(1 + \varepsilon)A_1 - (1 - \varepsilon)B_1 = 0, \quad (\text{A.17})$$

where  $\varepsilon = p/(\eta\alpha_D)$ . Applying the continuity conditions at  $z_D = d_D$  (Eqs. (A.10) and (A.11)), lead to

$$A_1 e^{\eta d_D} + B_1 e^{-\eta d_D} = \hat{s}_D^{(2)} \Big|_{z_D=d_D}, \quad (\text{A.18})$$

and

$$\eta(A_1 e^{\eta d_D} - B_1 e^{-\eta d_D}) = \frac{d\hat{s}_D^{(2)}}{dz_D} \Big|_{z_D=d_D}. \quad (\text{A.19})$$

Similarly, applying the no flow boundary condition at  $z_D = 1$  (Eq. (A.6)), leads to

$$\hat{s}_D^{(3)} = 2B_3 e^{-\eta} \cosh[\eta(1 - z_D)]. \quad (\text{A.20})$$

Continuity conditions at  $z_D = l_D$  lead to

$$2B_3 e^{-\eta} \cosh[\eta(1 - l_D)] = \hat{s}_D^{(2)} \Big|_{z_D=l_D}. \quad (\text{A.21})$$

$$-2\eta B_3 e^{-\eta} \sinh[\eta(1 - l_D)] = \frac{d\hat{s}_D^{(2)}}{dz_D} \Big|_{z_D=l_D}. \quad (\text{A.22})$$

For  $n = 2$ , solving Eq. (A.2) in Laplace–Hankel transform space, yields

$$\hat{s}_D^{(2)} = \hat{u}_D + \hat{v}_D, \quad (\text{A.23})$$

where

$$\hat{u}_D = \frac{C_D(1 - p\bar{\Phi}_{uc})}{\kappa\eta^2 \xi_w K_1(\xi_w)}. \quad (\text{A.24})$$

and

$$\hat{v}_D = A_2 e^{\eta z_D} + B_2 e^{-\eta z_D}, \quad (\text{A.25})$$

The five Eqs. (A.17)–(A.19), (A.21) and (A.22), together with Eq. (A.23) can be used to determine the five unknown coefficients  $A_1$ ,  $A_2$ , and  $B_1$ – $B_3$ . It can then be shown that

$$\hat{v}_D = -\frac{\hat{u}_D}{\Delta_0} \{ \Delta_1 \cosh[\eta(1 - z_D)] + \sinh(\eta l_D^*) [\cosh(\eta z_D) + \varepsilon \sinh(\eta z_D)] \}. \quad (\text{A.26})$$

The integral in Eq. (A.9) is

$$\frac{1}{b_D} \int_{d_D}^{l_D} \hat{s}_D^{(2)} dz_D = \hat{u}_D + \frac{1}{b_D} \int_{d_D}^{l_D} \hat{v}_D dz_D = \hat{u}_D + \langle \hat{v}_D \rangle. \quad (\text{A.27})$$

Substituting Eq. (A.26) into Eq. (A.27) leads to

$$\frac{1}{b_D} \int_{d_D}^{l_D} \hat{s}_D^{(2)} dz_D = \hat{u}_D (1 - \langle \hat{w}_D \rangle) \quad (\text{A.28})$$

where

$$\langle \hat{w}_D \rangle = \frac{1}{b_D \eta \Delta_0} [\Delta_1 \sinh(\eta d_D^*) + (\Delta_2 - 2\Delta_1) \sinh(\eta l_D^*)] \quad (\text{A.29})$$

$$\Delta_0 = \sinh(\eta) + \varepsilon \cosh(\eta)$$

$$\Delta_1 = \sinh(\eta d_D) + \varepsilon \cosh(\eta d_D)$$

$$\Delta_2 = \sinh(\eta l_D) + \varepsilon \cosh(\eta l_D)$$

$$\text{and } l_D^* = 1 - l_D, \quad d_D^* = 1 - d_D.$$

Taking the Laplace transform of Eq. (A.9) and replacing the integral on the left-hand-side with Eq. (A.28), gives

$$(p^2 + \beta_1 p + \beta_2) \bar{\Phi}_{uc} - p - \beta_1 = (1 - p\bar{\Phi}_{uc}) \bar{\Omega} / 2 \quad (\text{A.30})$$

where  $\bar{\Omega}$  is defined in Eq. (18). Solving the above equation for  $\bar{\Phi}_{uc}$  yields the required source well response in Laplace transform space.

## References

- Barrash, W., Clemo, T., Fox, J.J., Johnson, T.C., 2006. Field, laboratory, and modeling investigation of the skin effect at wells with slotted casing, Boise Hydrogeophysical Research Site. *Journal of Hydrology* 326, 181–198.
- Barrash, W., Reboulet, E., 2004. Significance of porosity for stratigraphy and textural composition in subsurface, coarse fluvial deposits: Boise Hydrogeophysical Research Site. *Geological Society of America Bulletin* 116, 1059–1073. doi:10.1130/B25370.1.
- Bohling, G.C., Butler Jr., J.J., Zhan, X., Knoll, M.D., 2007. A field assessment of the value of steady-shape hydraulic tomography for characterization of aquifer



- heterogeneities. *Water Resources Research* 43 (W04530). doi:[10.1029/2006WR004932](https://doi.org/10.1029/2006WR004932).
- Bouwer, H., Rice, R., 1976. A slug test for determining hydraulic conductivity of unconfined aquifers with completely or partially penetrating wells. *Water Resources Research* 12 (3), 423–428.
- Bredehoeft, J.D., Papadopoulos, I.S., 1980. A method for determining the hydraulic properties of tight formations. *Water Resources Research* 16 (1), 233–238.
- Butler Jr., J.J., 1998. *The Design, Performance and Analysis of Slug Tests*. Lewis Publishers, Boca Raton.
- Butler Jr., J.J., 2002. A simple correction for slug tests in small-diameter wells. *Ground Water* 40 (3), 303–307.
- Butler Jr., J.J., Zhan, X., 2004. Hydraulic tests in highly permeable aquifers. *Water Resources Research* 20, W12402.
- Cardiff, M., Barrash, W., Thoma, T., Malama, B., 2011. Information content of slug tests for estimating hydraulic properties in realistic, high-conductivity aquifer scenarios. *Journal of Hydrology* 403 (1–2), 66–82.
- Cooper, H.H.J., Bredehoeft, J.D., Papadopoulos, I.S., 1967. Response of a finite-diameter well to an instantaneous charge of water. *Water Resources Research* 3 (1), 263–269.
- de Hoog, F.R., Knight, J.H., Stokes, A.N., 1982. An improved method for numerical inversion of Laplace transforms. *SIAM Journal of Scientific and Statistical Computing* 3 (3), 357–366.
- Doherty, J., 2002. *Manual for PEST*. Watermark Numerical Computing, 5th Ed. Australia.
- Fox, J.J., 2006. Analytical modeling of fully penetrating pumping tests at the Boise Hydrogeophysical Research Site for aquifer parameters and wellbore skin. Master's thesis, Boise State University, Boise, ID.
- Hyder, Z., Butler Jr., J.J., McElwee, C.D., Liu, W., 1994. Slug tests in partially penetrating wells. *Water Resources Research* 30 (11), 2945–2957.
- Kipp Jr., K.L., 1985. Type curve analysis of inertial effects in the response of a well to a slug test. *Water Resources Research* 21 (9), 1397–1408.
- McElwee, C.D., Zenner, M.A., 1998. A nonlinear model for analysis of slug test data. *Water Resources Research* 34 (1), 55–66.
- McGuire, V.L., 1994. Characterizing vertical distribution of horizontal hydraulic conductivity in an unconfined sand and gravel aquifer using double packer slug tests. Master's thesis, University of Nebraska, Lincoln.
- Moench, A.F., 1997. Flow to a well of finite diameter in a homogeneous, anisotropic water table aquifer. *Water Resources Research* 33 (6), 1397–1407.
- Moench, A.F., Garabedian, S.P., LeBlanc, D.R., 2001. Estimation of hydraulic parameters from an unconfined aquifer test conducted in a glacial outwash deposit, Cape Cod, Massachusetts. US Geological Survey, Professional Paper 1629.
- Neuman, S.P., 1972. Theory of flow in unconfined aquifers considering delayed response of the water table. *Water Resources Research* 8 (4), 1031–1045.
- Springer, R.K., Gelhar, L.W., 1991. Characterization of large-scale aquifer heterogeneity in glacial outwash by analysis of slug tests with oscillatory response, Cape Cod, Massachusetts. *Water Res. Invest. Rep.* 91-4034, US Geological Survey.
- Zenner, M.A., 2009. Near-well nonlinear flow identified for various-displacement well response testing. *Ground Water* 47 (4), 526–533.
- Zlotnik, V.A., McGuire, V.L., 1998. Multi-level slug tests in highly permeable formations: 1. Modifications of the Springer-Gelhar (SG) model. *Journal of Hydrology* (204), 271–282.
- Zurbuchen, B.R., Zlotnik, V.A., Butler Jr., J.J., 2002. Dynamic interpretation of slug tests in highly permeable aquifers. *Water Resources Research* 38 (3), 1025. doi:[10.1016/j.jhydrol.2007.08.018](https://doi.org/10.1016/j.jhydrol.2007.08.018).